CrystEngComm

HIGHLIGHT

View Article Online
View Journal | View Issue

CrossMark click for updates

Cite this: *CrystEngComm*, 2017, **19**, 1143

A review on recent advances for nucleants and nucleation in protein crystallization

Ren-Bin Zhou,[a] Hui-Ling Cao,*[b] Chen-Yan Zhang[a] and Da-Chuan Yin*[a]

Received 14th December 2016,
Accepted 25th January 2017

DOI: 10.1039/c6ce02562e

rsc.li/crystengcomm

The elucidation of protein structures by X-ray crystallography remains the most effectual method to provide accurate structural details at atomic resolution for rational drug design and other biotechnological research studies. Also, emerging applications of protein crystals as ordered nanostructure scaffolds for catalysis, imaging, and drug delivery are attracting much attention. However, the first step of these applications is obtaining high-quality crystals, which is still an obstacle. Successful crystallization requires two steps: nucleation and crystal growth, while the nucleation is a precondition for harvesting the crystal of interest. So controlling protein nucleation may be an alternative breakthrough for this bottleneck. It is well known that nucleants can induce protein crystallization and improve crystal quality, so investigation on the nucleants that can be universally used for any protein crystallization is ongoing. This manuscript reviews the advances that have been achieved using nucleants in protein crystallization and it is a suitable reference for practical crystallization.

Published on 25 January 2017. Downloaded on 9/24/2024 11:26:54 PM.

1. Introduction

In recent decades, there has been increasing interest in understanding the basic mechanisms of biological processes by determining the 3D structures of proteins at the atomic level using X-ray diffraction (XRD).[1–4] However, the process of obtaining high-quality crystals for structural determinations is a bottleneck for this method, which delays and often hinders protein crystallography.[5–7] Based on the statistics, the likelihood of obtaining high-quality diffraction crystals from purified proteins has been stagnant at approximately 20% for decades.[8] The main challenge for protein crystallization is not the inability to obtain protein crystals. What's more disappointing is that the obtained crystals often cannot be used for structural determinations because of their inferior

[a] *Key Laboratory for Space Bioscience & Biotechnology, School of Life Sciences, Northwestern Polytechnical University, Xi'an, Shaanxi, PR China. E-mail: yindc@nwpu.edu.cn*
[b] *Shaanxi Key Laboratory of Ischemic Cardiovascular Disease, Institute of Basic & Translational Medicine, Xi'an Medical University, Xi'an, Shaanxi, PR China. E-mail: caohuiling_jzs@xiyi.edu.cn*

Ren-Bin Zhou

Ren-Bin Zhou received his bachelor degree in Biomedical Engineering at Northwestern Polytechnical University (Xi'an, China) in 2013. He is currently a Ph.D student at Northwestern Polytechnical University (Xi'an, China). His research interests include protein crystallization and structural biology.

Hui-Ling Cao

Hui-Ling Cao obtained her Ph.D in structure biology direction at Northwestern Polytechnical University (Xi'an, China) in 2013. In 2014, she obtained a vice professor position at the Institute of Basic & Translational Medicine, Xi'an Medical University. She also serves as a vice director in Shaanxi Key Laboratory of Ischemic Cardiovascular Disease. She has been researching structure biology and protein crystallization since 2009. Her research interests include protein crystallogenesis, structure biology and drug discovery concerning cardiovascular diseases and cancer. Now she is the author of 30 research papers and presides over five research funds with more than one million RMB.

Published on 25 January 2017. Downloaded on 9/24/2024 11:26:54 PM.

qualities. Multiple advanced methods have been proposed to overcome this obstacle by inducing crystal formation and improving crystal quality. These methods involve controlling the factors that affect protein crystallization (*i.e.*, protein concentration,[9] crystallization temperature,[10,11] pH value,[12] precipitant,[13] buffer, additive,[14] detergent), utilizing special environments (*i.e.*, microgravity,[15] magnetic fields,[16,17] electric fields,[18] stirring[19]), developing innovative crystallization methods (microfluidic platforms[20]), pursuing efficient protein screening kits,[21] and so on. All these methods have been proved with varying degrees of success.[7] However, the ultimate goal is to characterize a method that is suitable for all protein-to-crystal attempts, where the crystal quality is high enough for diffraction data collection.

Nucleants induce protein heterogeneous nucleation and improve crystal diffraction resolution in a controlled manner by providing a substrate to induce nucleation, which subsequently accelerates crystal growth.[22] A 1988 study was the first to reveal that nucleation is induced when minerals are used as heterogeneous nucleants.[23] It has since been demonstrated that numerous materials (*i.e.*, zeolites, mica and hair) can induce protein nucleation for individual proteins with varying degrees of success, though they cannot be universally used. Investigations on multiple substances as 'universal' nucleants for protein nucleation are ongoing. These agents include: (1) mineral substrates for epitaxial nucleation; (2) poor quality crystals or microcrystals for seeding; (3) charged surfaces (*i.e.*, functionalized mica, chemically modified mica, poly-L-lysine surfaces and polymeric film) inducing nucleation by specific interactions; (4) porous nucleants (*i.e.*, porous silicon, bioactive gel-glass, carbon-nanotube-based materials, engineered nano-confined spaces, low density porous or non-porous polystyrene divinylbenzene microspheres (SDB), nanoporous gold nucleants, mesoporous 3D nanotemplates); (5) natural nucleants with their superior biocompatibilities (*i.e.*, minerals, dried seaweed, horse hair, cellulose, hydroxyapatite); (6) the LB nanotemplate (a protein-based nucleant known as the Langmuir–Blodgett homologous protein thin film template) and porous nucleant MIPs (molecularly imprinted polymers). Each nucleant has enabled the attainment of multiple resistant to crystallization crystals and has improved several inferior qualities of the crystals for data collection.

This review starts with a brief assessment of the theoretical issues that surround nucleation and nucleants, including classical nucleation theory, two-step nucleation theory, and the roles and mechanisms of heterogeneous nucleants. Six nucleant types are described based on their detailed mechanisms and specific applications toward protein crystallization. LB nanotemplates and MIPs are novel and effective nucleants and are solely reviewed based on their applications toward inducing nucleation and improving the crystal quality, preparation and mechanism. Lastly, a succinct conclusion is drawn and practice suggestions are provided. This paper is a suitable reference for practical crystallization.

2. Theoretical issues surrounding nucleation and nucleants

2.1 Nucleation theory

An energy barrier must be overcome to form the preliminary crystal nucleus. Crystal nucleation primarily depends on a solution's supersaturation level. Supersaturation, the driving force behind crystallization, signifies that a solution contains the maximum number of dissolved molecules under a given condition at the thermodynamic equilibrium. Because the solid (crystalline) state is more stable than the liquid state (which decreases the Gibbs free energy of the system), supersaturation spontaneously drives the formation and deposition of droplet-like molecular clusters.[24,25]

Gibbs has described the free energy changes that occur within the thermodynamic equilibrium process throughout nucleation. Classical nucleation theory proposes that the free energy of nucleation is associated with two free energies. The

Chen-Yan Zhang

Chen-Yan Zhang, Ph.D, associate professor at Northwestern Polytechnical University, majored in protein crystallization methodology and protein structure biology.

Da-Chuan Yin

Da-Chuan Yin obtained his Ph.D in Materials Science at Northwestern Polytechnical University (Xi'an, China) in 1996. He became a lecturer at Northwestern Polytechnical University in 1997. In 2006 he obtained a professor position at the School of Life Sciences, Northwestern Polytechnical University. He has been researching protein crystallization since 2000. Now he is the author of more than 80 scientific research papers and 20 patents. His research interests include protein crystallogenesis, utilization of high magnetic fields for materials processing, and biomedical materials for cell cultures and tissue engineering.

 This journal is © The Royal Society of Chemistry 2017

Published on 25 January 2017. Downloaded on 9/24/2024 11:26:54 PM.

negative term is the energy required for bonds to form between molecules in the crystals; this is known as the volume free energy (ΔG_v). The positive term corresponds to the unsatisfied bonds that are present on the crystal's surface; this is known as the surface free energy (ΔG_s).[26] Therefore, the free energy required for nucleation (ΔG) is the sum of the free energy change for the phase transformation (ΔG_v) and the free energy change for the surface formation (ΔG_s). When nucleation begins, the nuclear volume grows at a minor rate compared to the surface volume till reaching the maximum (ΔG critical) in which the situation changes. Then the nuclear volume grows faster than the nuclear surface volume producing a negative value of the Gibbs free energy, making this process spontaneous. Thus, ΔG_v prevails and promotes molecular cluster formation. At the same time, an increase in the free energy of the solid/liquid interface favors dissolution. Therefore, molecular cluster formation depends on the competition between a decrease in ΔG_v and an increase in ΔG_s, as shown in Fig. 1. The Gibbs free energy for nucleation (ΔG) is a function of the cluster size (r). When it is small, the increasing ΔG promotes dissolution of molecular clusters. As the cluster size increases, ΔG reaches its maximum value and subsequently decreases. This molecular cluster size is known as the critical size. When it is exceeding the critical size, molecular cluster growth becomes energy-favorable and results in nucleation.[27]

2.1.1 Classical nucleation theory. Classical nucleation theory, the simplest and most commonly used theory, describes the protein nucleation process. It postulates that considerable fluctuation of the solution concentration forms unstable and ordered droplet-like molecular clusters, whose accumulation modes are similar to crystals. The ordered molecular clusters subsequently develop into crystal nuclei and then grow to form a crystal, as shown in Fig. 2.

2.1.2 Two-step nucleation theory. Several shortcomings of classical nucleation theory have emerged. First, it overestimates the crystal nucleation rate by 10 orders of magnitude above the predicted value. Second, nucleation is temperature-independent during the supersaturation increase.[28] Based on recent studies and simulations, several researchers have proposed the two-step nucleation theory. The first step of crystal nucleation comprises the formation of a disordered protein-rich dense droplet; the second step comprises the reassembly of the disordered proteins and the formation of ordered crystal nuclei inside the droplet,[29–31] as shown in Fig. 2. If the dense droplet is stable, crystal nucleation occurs inside the macroscopic droplet, and the formation of ordered nuclei can be directly observed.[32,33] The dense droplet is usually unstable and is under a higher free energy than a dilute droplet. The metastable molecular clusters contain protein-rich dense droplets and crystal nuclei that are formed from the dense droplets.[34,35] These protein-rich droplets have been observed during the crystallization of several proteins, including lysozyme,[36,37] glucose isomerase,[38] and hemoglobin A and S,[39] and have proven their key role in crystal nucleation.[40,41] Additionally, crystal nucleation has been directly observed inside similar mesoscopic clusters in colloids.[42] Although the two-step nucleation theory was initially proposed for protein crystallization, recent experimental and theoretical studies have demonstrated that it also applies to macromolecules and small organic molecules.[27]

2.1.3 Heterogeneous nucleation theory. The classical nucleation theory and two-step nucleation theory are indeed relevant and essential to explain the phenomenal observations, but heterogeneous nucleation theory cannot be naively ignored. Heterogeneous nucleation can be considered as a surface or particle assisted nucleation process, even supersaturation is insufficient for homogeneous nucleation.[43] In realistic situations, container walls and impurities are usually present and hence crystallization occurs by heterogeneous nucleation.[44] The heterogeneous nucleation theory proposes that the surfaces can absorb or specifically interact with the protein molecules, which then creates a higher local

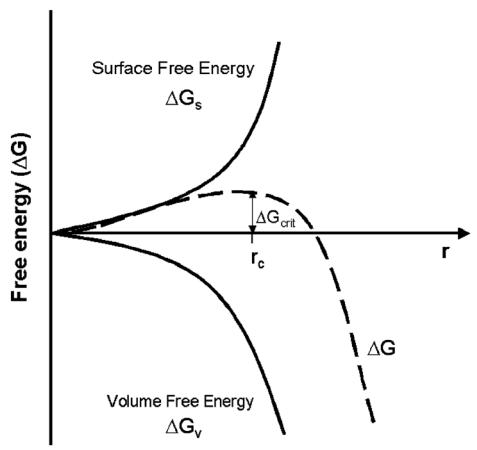

Fig. 1 Free energy diagram for nucleation. Reprinted with permission.[27] Copyright 2009, American Chemical Society.

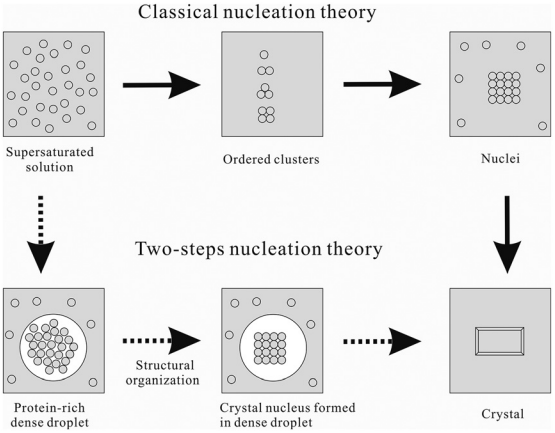

Fig. 2 Crystal nucleation mechanism, classical nucleation theory and two-step nucleation theory. Solid arrows indicate the classical nucleation theory: the ordered clusters occur directly from the supersaturated solution and grow into nuclei. Dashed arrows represent the two-step nucleation theory: disordered protein-rich dense droplet forms, and then crystal nuclei may form inside the droplet.

Published on 25 January 2017. Downloaded on 9/24/2024 11:26:54 PM.

concentration of protein and favors the formation of pre-nucleation clusters.[45,46] Once these pre-nucleation clusters have formed then the heterogeneous surfaces stabilize them, eventually favoring their transition to crystal nuclei.[47] Alternatively, the heterogeneous nucleation is energetically favored compared with the homogeneous nucleation, because there is an overall reduction of the interfacial energy of the crystal nuclei, thus the critical size of nuclei is smaller and more stable for crystal formation.[23,48] Last but not the least, the most obvious role of heterogeneous nucleation is stabilizing the necessary intermediary to the right crystal structure,[49] which is similar to the way enzymes can stabilize the transition state of substrates but don't influence the final product of the catalyzed reaction. In the following parts, nucleants that induce heterogeneous nucleation are comprehensively addressed.

2.2 Mechanism of promoting nucleation with nucleants

Successful crystallization requires two steps: nucleation and crystal growth. Nucleation is the first major step for crystallization and includes homogeneous and heterogeneous nucleation. Homogeneous nucleation is a random process. Multiple critical nuclei are formed when enough target protein molecules simultaneously assemble in the same region inside the crystallization drop, indicating that homogenous nucleation occurs at higher supersaturation levels. Generally, the energy barrier is low when supersaturation is high, which facilitates the formation of the critical nuclei. However, extremely high supersaturation levels accelerate the crystallization speed, which introduces unfavorable effects, such as structural defects and excessive nucleation, then lead to numerous small crystals instead of a few large ones. Meanwhile, heterogeneous nucleation is often promoted by other substrates and crystallization can be conducted in a controlled manner under metastable conditions.[50]

Nucleants, such as particles or surfaces, can induce heterogeneous nucleation to promote crystallization. To date, a variety of materials have been demonstrated as efficient nucleants, ranging from minerals to porous materials, protein-based and non-protein-based ones, and modified surfaces and natural ones. Generally, it is more advantageous for a protein molecule to be added to an existing nucleus than to form a new nucleus. Also, the pre-existing nucleants lower the energy barrier of the system and stabilize the formed nuclei. In detail, various nucleants may affect heterogeneous nucleation through different mechanisms. For example, minerals as nucleants are for epitaxial nucleation, which requires a match between the crystal lattice of the minerals and that of the protein crystal.[23,51] The charged surfaces facilitating nucleation are mainly by electrostatic interactions.[52,53] The porous materials can trap protein molecules to form a high local supersaturation to induce nucleation.[54] The LB nanotemplate is thought to assist nucleation by causing high electrostatic potential at the film surface, which attracts protein molecules from the solution.[55] Meanwhile, a MIP can attract enough protein molecules to overcome the energy barrier for the first step nucleation.[56] At the same time, the roughness, topography, microstructure and physicochemical properties of the nucleants affect the heterogeneous nucleation.[57]

3. Classification and application of nucleants

3.1 Seeding

Seeding is a valuable method for obtaining high-quality crystals of target proteins when regular attempts fail. It is a common practice to transfer several small crystals of the same or different protein as "seeds" under similar or identical crystallization conditions to induce high-quality crystal formation. Seeding can be performed using a cognate protein or by cross-seeding with a different protein.

3.1.1 Seeding (cognate protein). There are three types of seeding: (1) macro-seeding, where single crystals are transferred as seeds; (2) micro-seeding, where the actual seeds are invisible and transferred under a microscope; (3) streak seeding, where a wand (usually, an animal whisker) is used to transfer seeds that contain crystals into a new crystallization drop.[58–61]

The seeds are visible in macro-seeding, and the seeding procedure is as follows: (1) a suitable single crystal is selected as the seed and collected with a crystal loop from the drop; (2) the crystal is repeatedly washed in a stable mother solution; (3) the washed crystal is transferred to a new crystallization drop for crystallization.[61]

The seeding procedure for micro-seeding differs from that of macro-seeding and proceeds as follows: (1) multiple small crystals with insufficient qualities in the mother solution are smashed using sonication, by vortexing or with glass rods; (2) the smashed crystals are transferred into a new crystallization drop for crystallization with a seeding needle or micropipette tip. The serial dilution method is used to determine the ideal seeding concentration.[62,63]

Streak seeding is the easiest and fastest of the three methods. An animal whisker (cat, rabbit or horse hair) is typically used as a seeding wand, which traps the nuclei by it touching the mother crystallization solution.[64] A streak line then forms a new drop with the whisker, and the trapped seeds deposit along the streak line.[61] Finally, the crystals grow along the streak line, as shown in Fig. 3.

In summary, the advantages of the seeding methods are obvious. For example, seeding can be utilized to obtain larger and higher diffraction-quality single crystals as well as improve the success rate of protein crystallization,[65,66] including membrane proteins.[67] Moreover, its facilitation of new crystallization hits is less time-consuming. However, obtaining protein crystals is the precondition for seeding. Recently, automated devices have been developed for seeding trials,[63] but they are only employed for primary crystallization screening; crystallization optimization through seeding continues to be manually performed.

 This journal is © The Royal Society of Chemistry 2017

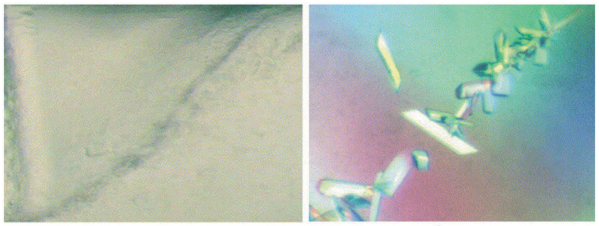

Fig. 3 Streak seeding of the mycobacterium tuberculosis RV 2465c protein. (a) Accumulated precipitates along the streak line. (b) Crystals along the streak line. Reprinted with permission.[61] Copyright 2003, Elsevier Science (USA).

Published on 25 January 2017. Downloaded on 9/24/2024 11:26:54 PM.

3.1.2 Cross-seeding (different proteins). In some cases, crossing-seeding (seeding with a variant of the target protein or the homologous protein) may be successful.[68] This strategy can be used for related proteins including complexes with various ligands, heavy-atom derivatives,[69] and the proteins with similar structures such as the Fab fragments of antibodies. For example, upon crystallization of sixteen human antibody Fab fragments, in the initial screening, only three Fab fragments provided diffraction-quality crystals, eight Fab fragments provided hits that required optimization, and five Fab fragments failed to give hits. Application of the crystals of the three Fab fragments to cross-seeding resulted in the structural determination of all sixteen Fab fragments.[70] If no crystals were produced in the initial screening, the seeds obtained from the easily crystallized protein can be attempted by cross-seeding. It was reported that a mixture of fifteen unrelated easily crystallized proteins by cross-seeding gave crystallization hits in two test target proteins.[71] The procedure of cross-seeding is identical to the seeding procedure described above, but a stable mother liquid (such as 100% PEG600) must be screened before seeding.

3.2 Natural nucleants

Natural nucleants are the preferred heterogeneous nucleants because they have suitable biocompatibilities and are easily obtained. Mineral surfaces comprise the earliest reported natural nucleants, having been described by Alexander Mcpherson and Paul Shlichta in 1988.[23] They tested fifty different mineral samples as nucleants for the crystallization of four model proteins—canavalin, concanavalin, catalase B and lysozyme. Their results showed that the mineral substrates induced nucleation and accelerated crystal growth for the four proteins. It is noteworthy that nucleation occurred earlier, at a lower critical supersaturation. Moreover, the mineral substrates altered the crystal habit and unit cell properties. For example, catalase crystals varied from the fine trigonal to the orthorhombic laths. For lysozyme, both the dominant single tetragonal crystals and the fine needle crystals were observed in the presence of the mineral substrates. Regarding unit cell properties, the traditional crystal form of concanavalin B is hexagonal with the space group $P6_3$, but a new orthorhombic symmetry $P2_12_12_1$ was evident with the mineral substrates.[24] The match degree between the mineral substrates and the protein crystal lattices may play an important role in promoting nucleation.[51]

Nine potential natural nucleants have subsequently been tested for the crystallization of ten model proteins in a sparse matrix screen.[72] The results showed that four natural nucleants, including dried seaweed, horse hair, cellulose and hydroxyapatite, have positive effects on crystallization. The most efficient natural nucleant was dried seaweed. Predictably, the use of multiple nucleants in the same drop produced the best results. Nonetheless, there were two natural nucleants (fumed silica and carboxymethyl sephadex) that negatively affected crystallization. Positive nucleants for some proteins may act as negative inhibitors for others.

Hair, particularly horse hair and rat whiskers, has been successfully used as a heterogeneous nucleant for many years. It was initially used as a tool for streak seeding; the nucleation-inducing properties of hair itself were discovered by chance. The nucleation-inducing properties of horse hair have been subsequently investigated for three model proteins and a resistant-crystallized recombinant protein, the Fab-D protein. Preliminary investigation demonstrated that horse hair positively affected nucleation at the beginning of the crystallization process.[60] Subsequent investigation of human hair fragments as nucleants for the crystallization of three model proteins (lysozyme, glucose isomerase and a polysaccharide-specific Fab fragment) and a resistant-crystallized protein without a 3D structure (the potato serine protease inhibitor) has proved that human hair was a suitable nucleant for obtaining potato protease inhibitor crystals.[73]

To investigate the mechanistic basis of the hair surface as a nucleant, the following three hair surface properties have been studied: (1) keratins, the most predominant protein in hair; (2) the lipids on the hair surface; and (3) the surface structure and its overlapping terraces. The delipidifying treatment of hair with petroleum ether as the delipidifying agent did not influence crystallization, but the denaturing treatment of hair with ethanol and sodium hydroxide did affect crystallization. Furthermore, an artificial polymer replica for hair did not show a clear preference for nucleation. It is likely that the keratins on the hair surface are essential for crystallization.

3.3 Charged surface

The aggregation of protein molecules is indispensable for nucleation. Protein molecules become charged when they are subjected to specific conditions. This is a useful property because protein molecules can be attracted using an oppositely charged substrate as a nucleant for an electrostatic interaction. In practice, charged surfaces are designed as nucleants to promote protein crystallization. For example, functionalized mica with negatively charged sulfonated polystyrene films and positively charged silanized sheets were prepared

Published on 25 January 2017. Downloaded on 9/24/2024 11:26:54 PM.

as charged nucleants to promote the crystallization of insulin and ribonuclease A.[74] As expected, the charged surface shortened the crystallization time and minimized protein consumption. The interactions between the charged surface and the protein molecules enrich the protein molecules around the charged surface to reach local supersaturation, which favors nucleation and crystal growth.[43,75] Additionally, the weak force of the charged surface stabilizes the formed nuclei.

The fluorinated layered silicate surface has been used as a crystallization nucleant; it promoted lysozyme nucleation while silicates without fluorine suppressed nucleation.[76] Nucleation promotion was also observed when fluorine was replaced with hydroxyl groups. The fluorinated layered silicate surface has also been used to crystallize twelve proteins with a wide range of pIs and molecular weights; the negatively charged surface promoted protein nucleation regardless of the net charges and molecular weights of the proteins. The result of the initial screening trials with fluoro-substituted saponite has verified the beneficial effects, which included increasing the initial screening success rate, reducing the nucleation energy barrier and minimizing protein consumption. The mechanism may involve the interaction between the silicate's negatively charged fluorine atoms or hydroxyl groups and the positively charged residues of the protein molecules, which attracts protein molecules causing them to gather at the silicate surface where they form a high local supersaturation zone to form the initial critical nuclei.

Furthermore, chemically modified mica, poly-L-lysine (PLL) surfaces, polymeric films and patterned silicon have been reported as potential nucleants. PLL surfaces are positively charged surfaces that are coated with cationic polymerized lysine. They attract negatively charged molecules and repel the positive ones. The net charge of the lysozyme protein is also positive in the optimum experimental conditions. Because of the repulsive interaction, the PLL surface orients the single lysozyme crystals and diminishes the nucleation number, as shown in Fig. 4.[77] However, when negatively charged proteins were used, the PLL surface oriented the single crystals, but it did not affect the nucleation number for the tested proteins.[78]

Additionally, other charged polymeric surfaces (*i.e.*, sulfonated polystyrene, cross-linked gelatin films with adsorbed poly-lysine, and silk fibroin with entrapped poly-L-lysine or poly-L-aspartate) have been used as heterogeneous nucleants to crystallize concanavalin A and lysozyme. Compared with the siliconized cover glass and the charged polymeric surfaces, the surfaces reduced both the induction time and the necessary protein concentration for nucleation while increased the nucleation density to promote crystallization.[79]

3.4 Porous nucleants

3.4.1 Porous nucleants. The initial use of porous substrates–porous silicon as a nucleant was demonstrated in 2001. The crystals of five of six tested proteins have been successfully obtained from metastable solutions in the presence of porous silicon. The silicon pore size distribution (5–10 nm) is similar to the protein molecular sizes in the crystallization solution. Therefore, the silicon pores may trap the protein molecules and induce nucleation and crystal growth.[80]

New porous nucleants have since been developed and successfully proven for promoting protein crystallization. In 2006, mesoporous bioactive gel-glass, which contained a disordered porous medium with a pore size distribution of 2–10 nm, was developed for protein crystallization and became one of the most successful heterogeneous nucleants. The bioglass promoted the nucleation of various proteins, including multiple resistant-crystallized proteins. The use of the bioglass was more convenient than using porous silicon because it was easy to add the bio-glass into the crystallization drops.[43] The bio-glass has been commercialized as 'Naomi's Nucleant' by Molecular Dimensions.

Although bio-glass nucleants induced the crystallization of numerous proteins, its pore sizes and surface chemistry were not easily controlled. Thus, a carbon-nanotube-based material with a controlled pore size and surface chemistry was developed as an efficient nucleant in 2009, as shown in Fig. 5.

Another study investigated the effects of engineered nanoconfined spaces on protein crystallization, which had narrow pore size distributions (pore diameters of 3–4 nm, 6–8 nm, 10–12 nm, 13–15 nm and 17–21 nm) and highly ordered pore structures. Proteins with a wide range of molecular weights, from 14 kDa to 450 kDa, were utilized for the crystallization trials.[82] The results were as follows: the 3–4 nm pore

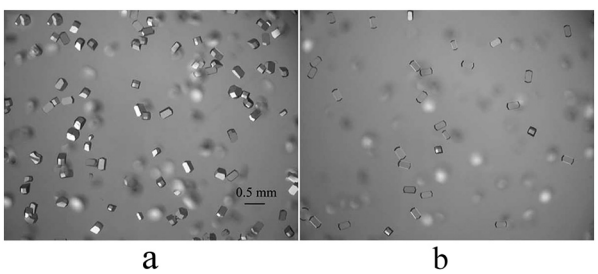

Fig. 4 The orientation and reduction of lysozyme crystals. (a) Crystals obtained on normal glass at lysozyme 30 mg ml^{-1}, NaCl 40 mg ml^{-1} and pH 4.5. (b) Crystals obtained on PLL-coated glass under the same conditions. Reprinted with permission.[77] Copyright 2002, Elsevier Science.

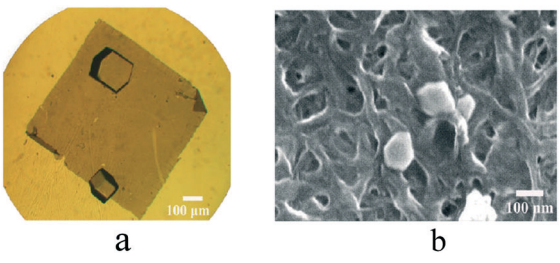

Fig. 5 (a) Optical microscopy image of lysozyme crystals on a sheet of transparent buckypaper (films of entangled carbon nanotubes). (b) SEM image of a lysozyme crystal too small to be visible *via* optical microscopy. Reprinted with permission.[81] Copyright 2009, American Chemical Society.

 This journal is © The Royal Society of Chemistry 2017

Published on 25 January 2017. Downloaded on 9/24/2024 11:26:54 PM.

diameter worked well for the 12–24 kDa protein crystallization, the 6–8 nm pore diameter was ideal for the 67 kDa protein crystallization, and the proteins with molecular weights of 106–232 kDa were successfully crystallized using the 10–12 nm pore size. The higher molecular weight protein (450 kDa) required a higher 17–21 nm pore size to crystallize. Thus, a wide range of pore sizes would broaden the ability to crystallize different proteins. Surprisingly, human serum albumin (HSA) and concanavalin A-type IV did not crystallize on the porous nucleants with broad pore size distributions,[80] while the narrow range pore size ones succeeded (HSA with the 3–4 nm pore diameter; concanavalin A with the 10–12 nm pore diameter). Additionally, the nucleants with slightly larger pore sizes than the gyration diameters of the proteins induced and stabilized the nuclei.[82]

Nanoporous gold nucleants have also been recently used as heterogeneous nucleants for protein crystallization. When the pore diameter of the nucleant was similar to the diameter of the protein molecule, nucleation on the nucleant surface may have occurred under supersaturation conditions that were milder than usual, which would result in a lower energy barrier for nucleation and higher quality crystals. The interaction between the surface of the dealloying nanoporous nucleant and the target protein molecules played the dominant role in inducing nucleation, rather than the entropy contributions to the free energy of crystallization.[83]

Low density porous or non-porous polystyrene divinylbenzene microspheres (SDB) are appropriate agents for simultaneously improving nucleation and crystal quality. SDB adsorbs protein molecules at high concentrations and desorbs protein molecules at low concentrations. Thus, the adsorption and desorption properties of SDB enable the formation of relatively high and relatively low concentration regions in the same solution; the high concentration region is favorable to nucleation. Up to a specific size, the nuclei settle in the low concentration region to grow high-quality crystals.[84]

Mesoporous 3D nanotemplates are also new and efficient heterogeneous nucleating surfaces for protein crystallization. One study became the first to show that concanavalin A and catalase produced different crystal habits under identical crystallization conditions when 3D nanotemplates were used as nucleants. However, the crystals with different crystal habits exhibited the same space group by XRD. The habit modification was the combined result of the porosity and chemistry properties of the 3D nanotemplate.[85]

3.4.2 The mechanism of nucleation by pore materials. Using computer simulation, Page and Sear have determined the nucleation rate to be higher on the porous surface compared to a flat surface,[86] but its detailed mechanism remains unclear.

The mechanism of nucleation by porous materials is likely explained by four properties. (1) The nanopores trap the protein molecules by diffusion and capillary action, and the protein molecules are restrained inside these pores, which results in a higher local supersaturation and nucleation. The critical nuclei attract the protein molecules causing them to gather and ultimately grow into crystals.[86,87] (2) The pore size plays a dominant role in the nucleation rate. Successful nucleation involves two successive processes: the nucleation of the pore filling and nucleation outside the pore under the bulk (homogeneous) conditions. The aforementioned computer simulation shows that the smaller pore size results in a slower nucleation rate outside the pore, and a larger pore size leads to a slower initial pore filling. Therefore, the pore size should be approximately equal to that of the critical nuclei to maximize the nucleation rate.[86] (3) The surface chemistry of the pore also contributes to crystal nucleation. The pore surface exhibits a weak chemical attraction and a subsequent weak interaction with the protein molecule to promote nucleation. The attractive interaction facilitates the formation of the high density phase, which is essential for nucleation in the two-step nucleation mechanism. The high density phase formation has been observed and characterized using the light-scattering technique.[88] Additionally, the attractive interaction stabilizes the half-formed nuclei.[82] (4) The pore traps and immobilizes the protein molecules within, and this lowers the free energy barrier for nucleation.[82] Therefore, the nanoscale pore improves the solution's thermodynamic stability, which is favorable for protein folding and nucleation. This was verified in 2006 with a molecular dynamics simulation and experiment.[89]

3.5 Langmuir–Blodgett thin film template

3.5.1 Applications of LB nanotemplate for crystallization. The Langmuir–Blodgett homologous protein thin film template (LB nanotemplate) was developed by Eugenia Pechkova in 2001.[90] A homologous protein thin film was made using the Langmuir–Blodgett technology and transferred to a cover glass to modify the traditional hanging drop vapor diffusion method for promoting crystallization. The hen egg white lysozyme was invoked as the model protein to assess this new approach. The results showed that the modified hanging drop method with the LB nanotemplate improved lysozyme's crystal quality and increased its crystal growth rate. At the same time, lysozyme, thaumatin, proteinase K and human insulin were selected to estimate the crystal quality using the LB nanotemplate and microgravity.[91] Compared with the crystals from microgravity, the crystals obtained using the LB nanotemplate exhibited higher resolutions, greater numbers of reflections, lower water contents and lower B factors, which indicated higher qualities. Another study compared the LB nanotemplate method with the traditional hanging drop vapor diffusion method using six model proteins, including lysozyme, insulin, thermolysin, thaumatin, ribonuclease A and proteinase K. Compared with the traditional method, the LB nanotemplate facilitated protein nucleation, accelerated the crystal growth rate, and decreased the critical concentration for nucleation.[92]

Surprisingly, the LB nanotemplate successfully crystallized proteins whose structures had not previously been resolved,

Published on 25 January 2017. Downloaded on 9/24/2024 11:26:54 PM.

including bovine cytochrome P450 scc[93] and human protein kinase CKII alpha subunit.[94] Thus, the novelty and effectiveness of the LB nanotemplate method have generated increasing interest, which is evidenced by its prolific development.[87,92,93,95–98]

Multiple advanced techniques have been employed to evaluate the LB nanotemplate, including atomic force microscopy,[99] Raman spectroscopy,[100] small-angle X-ray scattering,[101] computer simulation, molecular dynamics,[102] Fourier transform infrared (FTIR) spectroscopy, and circular dichroism.[99] Lysozyme exhibited a surprising thermal stability during the preparation of the LB nanotemplate, retaining its secondary structure until 200 °C; above 200 °C, the protein aggregated.[99] The LB nanotemplate promoted disulfide bond formation (at the S6–S127/S30–S115 position) and hydrogen bond formation in lysozyme, which makes stable crystals easy to obtain.[100] Additionally, crystals that were obtained using the LB nanotemplate were highly resistant to radiation damage.[103]

3.5.2 Preparation of the LB nanotemplate. The following protocol is used to prepare the LB nanotemplate: (1) a protein solution is poured into a Langmuir–Blodgett trough with distilled water or a suitable buffer solution as a sub-phase. After spreading, a protein monolayer is immediately compressed at the desired surface pressure (depending on the nature of the protein) using the Langmuir–Blodgett technology. (2) The protein thin film is transferred from the sub-phase surface onto a cover glass. (3) The cover glass, which contains the protein thin film, is used for crystallization with the vapor diffusion method, as shown in Fig. 6.

3.5.3 The LB nanotemplate mechanism. There are two drivers of the LB nanotemplate mechanism. (1) The protein in the LB nanotemplate is directly transferred to the crystallization drop to participate in nucleation and crystallization. This has been proved using a prepared LB nanotemplate with a fluorescein-labelled protein, by ^{1}H NMR spectrometry and by mass spectrometry.[104] This phenomenon has also been modelled by a dynamic mathematical method.[102] (2) The increased surface pressure results in the increased anisotropy of the LB nanotemplate and protein molecule orientation to promote nucleation and crystallization,[105] which causes a dipole moment in the LB nanotemplate. The surface potential is −0.2 mV in the self-assembly (randomly oriented proteins), but is −80 mV (ordered and oriented proteins) in the LB template.[106] The dipole moment in the LB nanotemplate causes the uniform deposition of protein molecules in the LB film, which is beneficial to protein nucleation and crystallization.[98]

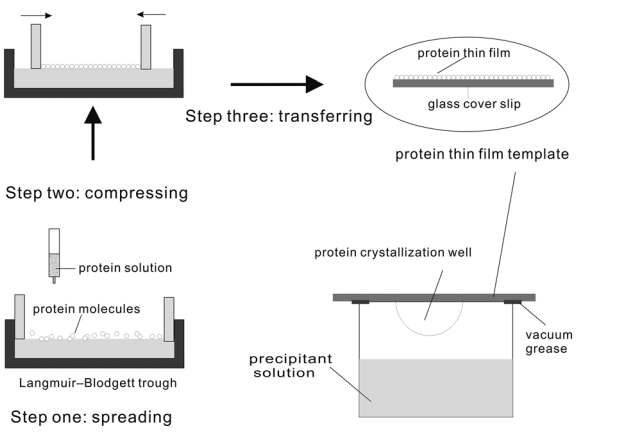

Fig. 6 Schematic of preparing the LB nanotemplate.

3.6 Molecularly imprinted polymers (MIPs)

3.6.1 Application of MIP for crystallization. MIPs produce molecularly selective sites *via* polymerization of a functional monomer and template molecule. The functional monomer interacts with the template molecule by hydrogen bonding and by weak Van der Waals forces. Once polymerized, the template molecules become trapped sin the polymer. After removal of the template molecules, the highly selective cavities remain, and they can remember the cognate template molecule and rebind to a non-cognate molecule of a similar shape and size.[107–109] MIPs have been successfully applied to small molecule studies.[110,111] Recently, the imprinting of biological macromolecules, including proteins and DNA, has generated interest.[112] However, MIPs cannot completely imitate the small molecule imprinting method because small molecules are stable in an organic solvent while proteins denature under identical conditions.[110] Therefore, a water-based imprinting system is a better choice. One report has shown that cross-linked acrylamide provides numerous advantages for protein imprinting.[113] Its polymer networks exhibit superior selectivity for template proteins compared with a non-imprinted acrylamide control, and it has successfully been used in protein separation and purification studies.[114,115] Furthermore, MIPs have commonly been applied to chemical sensors,[116] catalysis,[117] drug delivery,[118] biological antibodies, and receptor systems.[119]

In 2011, Naomi E. Chayen became the first to develop a water-based MIP (HydroMIP) as a non-protein nucleant for protein crystallization.[120] It is also known as a "smart material" because the MIPs are effective toward increasing the crystal hit number and improving crystal quality.[56] Seven proteins—lysozyme, trypsin, catalase, hemoglobin, intracellular xylanase IXT6-R217W, alpha crustacyanin, and human macrophage migration inhibitory factor (MIF)—have been used to evaluate the nucleation-inducing properties of the MIPs. Compared with the non-imprinted polymers and the control without polymers, MIPs induced protein nucleation through their cognate MIP and through other non-cognate MIPs of similar sizes in metastable conditions. Additionally, the diffraction qualities of the crystals that were obtained from the MIPs were superior to that of the control. For example, the complex HIV protein crystals showed diffraction up to 4.2 Å in the presence of lysozyme–MIP, but traditional methods failed to show crystal diffraction beyond 9 Å. Furthermore, the crystals appeared more quickly in the drops that contained MIPs above metastable conditions. Hemoglobin crystals have been

 This journal is © The Royal Society of Chemistry 2017

Published on 25 January 2017. Downloaded on 9/24/2024 11:26:54 PM.

observed after 5 days with 22.5% (wt/vol) PEG 3350 that contained Hemoglobin–MIP. At 25% (wt/vol) PEG 3350, all drops formed crystals, but they appeared after 7 days.[120,121]

To investigate MIP applications to initial screening experiments, four proteins have been screened with and without their cognate MIPs using the popular index screening kit. The useful crystals for two proteins, alpha crustacyanin and intracellular xylanase IXT6-R217W, have not been previously produced. The third protein, human macrophage migration inhibitory factor (MIF), required better resolution. An easily crystallized model protein, trypsin was used as the control.[120] The results showed that 8–10% of the screening trials of the aforementioned proteins produced hits, but these hits were missing in the absence of the MIPs. When the concentrations for the MIF and alpha crustacyanin were raised to 15–30%, the prior hits yielded crystals in the absence of MIPs. Thus, MIPs can screen new hits and decrease target protein consumption. Because MIPS are efficient and reproducible, they have been automated for applications in high-throughput robot-based screening trials.[122] Moreover, MIPs of differing molecular weights are commercially available for general use.

The MIP method has recently been improved by Chen's group.[123] The traditional precipitants were immobilized into MIPs to aid protein crystallization, and high-quality crystals of the flexible N-terminus of the human fragile X mental retardation protein were successfully obtained. The diffraction resolution was improved from 10 Å, which was typical of the traditional methods, to 3 Å when precipitant-immobilized MIPs were present.

Additionally, zwitterionic additives have been immobilized into MIPs to facilitate crystallization. Fortunately, the zwitterion-immobilized MIPs facilitated the formation of higher quality crystals in a shorter time compared with regular MIPs and traditional crystallization trials. The high-quality single crystals of a flexible protein, concanavalin A, have been successfully obtained using this approach.[124]

3.6.2 Preparation of MIPs. Because of their ease of preparation, high binding affinity and low cost, MIPs have been successfully used as nucleants for protein crystallization. MIPs are semiliquid nucleants. Thus, they are easily dispensed into the crystallization drops by automated robots without blocking the syringe needle. MIPs are prepared in the presence of functional monomers, cross-linkers and a template protein. Acrylamide-based polymers are inert, water compatible, economical, and easily produced and provide hydrogen bonds to interact with the template protein. Therefore, the acrylate family is suitable for use as MIPs.[125] Among members of the acrylate family, acrylamide (AA) is the most efficient imprinted functional monomer, followed by *N*-hydroxymethylacrylamide (NHMA) and *N*-iso-propylacrylamide (NiPAm).[126,127] The typical cross-linker is *N*,N_0-methylenebisacrylamide.

Semiliquid MIPs are prepared using a procedure that differs from that of the solid nucleants, as shown in Fig. 7. (1) A functional monomer (AA) and cross-linker (*N*,N_0-methylenebisacrylamide) are dissolved in deionized water.

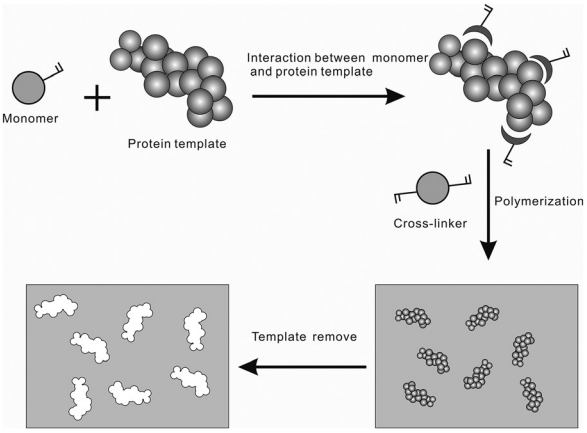

Fig. 7 Preparation of MIPs. Functional monomer (acrylamide) and template protein were polymerized by a cross-linker (*N*,N_0-methylenebisacrylamide). Then the template protein was removed by elution and protein specific cavities were left. Finally the target protein can be memorized by the complementary cavity and rebind to it to induce crystallization.

The template protein solution is then added to create the pre-MIP solution. (2) Ammonium persulphate (APS) and *N*,*N*,*N*,*N*-tetramethylethyldiamine (TEMED) are added to polymerize the solution at room temperature. (3) After polymerization, the formed gels are crushed. (4) The template protein molecule is eluted, and the complementary cavities remain. When the template proteins are introduced into a crystallization trial, they can be easily memorized and rebind to the cavities. The prepared MIPs are stored at 4 °C.[120]

3.6.3 The mechanism of MIP-induced protein crystallization. There are three main drivers of MIP-induced proteins crystallization. (1) The protein specific cavity in the MIP induces the protein molecules that are migrating near the MIP surface to form a protein-rich phase, which overcomes the energy barrier for the first nucleation step.[120,121] There are highly specific interactions between the MIP surface and cognate protein that do not occur with the traditional method, as evidenced by atomic force microscopy.[56,128] (2) The MIP cavities are complementary to the protein molecules, and they are randomly dispersed into the gel. Therefore, the cavities provide surfaces for protein molecule epitaxial growth.[120] (3) MIPs are porous materials, so the mechanisms of the porous materials described above can also be applied to MIPs.

4. Concluding remarks

4.1 Conclusion

(1) Seeding is a valuable way to obtain the high-quality crystals of target proteins when regular attempts fail.

(2) Natural nucleants, including minerals, dried seaweed, animal/human hair, cellulose and hydroxyapatite, are the preferred heterogeneous nucleants because they have suitable biocompatibilities and are easily obtained.

(3) Charged surfaces (*i.e.*, functionalized mica, chemically modified mica, poly-L-lysine surfaces, polymeric films) can

Published on 25 January 2017. Downloaded on 9/24/2024 11:26:54 PM.

stimulate protein molecule aggregation through their electrostatic interactions to promote protein nucleation and crystallization.

(4) The nanopores of porous nucleants can trap protein molecules to form a high local supersaturation to induce nucleation. Porous nucleants include porous silicon, bioactive gel-glass, carbon-nanotube-based materials, engineered nano-confined spaces, low-density porous or non-porous polystyrene divinylbenzene microspheres (SDB), nanoporous gold nucleants and mesoporous 3D nanotemplates. Bioactive gel-glass is a highly successful heterogeneous nucleant.

(5) The LB nanotemplate is a homologous protein thin film that is made using the Langmuir–Blodgett technology and is transferred to a cover glass to modify the traditional hanging drop vapor diffusion method to promote crystallization.

(6) The complementary cavities in MIPs can induce protein molecules to migrate toward the MIP surface and form a protein-rich phase to overcome the nucleation energy barrier.

4.2 Practical suggestions

To make full use of these nucleants, several practical suggestions are provided below. When crystals are obtained with qualities that are unsuitable for data collection, seeding is the ideal approach. When crystals cannot be obtained by trial and error, it is worth testing effective nucleants to increase the chances of inducing nucleation. The natural nucleants, which have better biocompatibilities and are easily obtained, increase successful crystallization outcomes. Specifically, a nucleant comprised of animal or human hair is the better choice for heterogeneous nucleation. Various porous nucleants are also made suitable by their effectiveness and convenience. They include porous silicon, bioactive gel-glass, carbon-nanotube-based materials, engineered nano-confined spaces, nanoporous gold nucleants and mesoporous 3D nanotemplates. Of the porous nucleants, bioactive gel-glass may be the better choice. Finally, universal nucleants, such as MIPs or LB nanotemplates, are also worth trying to increase the chances of obtaining crystals.

5. Future perspectives

Although these nucleants have been demonstrated to successfully aid protein crystallization, they are not so perfect and convenient for protein crystallization. For example, many nucleants only work with some certain cases not suitable for "general" use. The reported "universal" nucleants (LB template thin film and MIPs) also have some drawbacks. A special device is needed to fabricate the LB template thin film and can't be easily obtained in all the structural biology laboratories. Although the MIPs can conveniently yield and have been commercialized, effectively assist the crystallization of globular proteins, protein complexes and membrane proteins, it should notice that the MIPs nucleants can also facilitate salt crystallization when the crystallization buffer contains substantial levels of salt. So an important novel conclusion is to integrate all the nucleants' advantages (effects of epitaxy, special interactions and porous materials nucleation-promoting properties) into the design of more effective nucleants.

In the future, it is essential to achieve optimal universality of the heterogeneous nucleants for promoting any protein crystallization, with high automation to dispense them into the crystallization solution for high-throughput screen. Alternatively, the best strategy is to design functional crystallization plates for protein crystallization instead of introducing another heterogeneous nucleant.

Another aspect of protein nucleants that should be addressed is the theory explanation. This is possible to achieve by direct imaging. Scanning electron microscopy, atomic force microscopy and confocal fluorescence microscopy can be employed for this purpose. At the same time, computer simulation is a powerful tool to provide detailed information on nucleants aiding protein crystallization.

Competing interests

The authors have declared no competing interest.

Acknowledgements

This work was supported by the National Natural Science Foundation of China (Grant No. U1632126), the National Natural Science Foundation of China (Grant No. 11202167), the Fundamental Research Funds for the Central Universities (Grant No. 3102016ZY039), the Natural Science Foundation of Shaanxi Province, China (Grant No. 2016JM3012), and the Talents Program of Xi'an Medical University (No. 2015 RCYJ01).

Notes and references

1 H. P. Zheng, K. B. Handing, M. D. Zimmerman, I. G. Shabalin, S. C. Almo and W. Minor, *Expert Opin. Drug Discovery*, 2015, **10**, 975–989.
2 R. Giege, *FEBS J.*, 2013, **280**, 6456–6497.
3 A. R. Pearson and A. Mozzarelli, *Biochim. Biophys. Acta, Proteins Proteomics*, 2011, **1814**, 731–733.
4 J. L. Grey and D. H. Thompson, *Expert Opin. Drug Discovery*, 2010, **5**, 1039–1045.
5 J. A. Gavira, *Arch. Biochem. Biophys.*, 2016, **602**, 3–11.
6 A. Bijelic and A. Rompel, *Coord. Chem. Rev.*, 2015, **299**, 22–38.
7 I. Russo Krauss, A. Merlino, A. Vergara and F. Sica, *Int. J. Mol. Sci.*, 2013, **14**, 11643–11691.
8 N. E. Chayen and E. Saridakis, *Nat. Methods*, 2008, **5**, 147–153.
9 E. Saridakis, K. Dierks, A. Moreno, M. W. M. Dieckmann and N. E. Chayen, *Acta Crystallogr., Sect. D: Biol. Crystallogr.*, 2002, **58**, 1597–1600.
10 J. Liu, D. C. Yin, Y. Z. Guo, X. K. Wang, S. X. Xie, Q. Q. Lu and Y. M. Liu, *PLoS One*, 2011, **6**(3), e17950.
11 X. K. Wang, D. C. Yin, C. Y. Zhang, Q. Q. Lu, Y. Z. Guo and W. H. Guo, *Cryst. Res. Technol.*, 2010, **45**, 479–489.

 This journal is © The Royal Society of Chemistry 2017

Published on 25 January 2017. Downloaded on 9/24/2024 11:26:54 PM.

12 C. Y. Zhang, Z. Q. Wu, D. C. Yin, B. R. Zhou, Y. Z. Guo, H. M. Lu, R. B. Zhou and P. Shang, *Acta Crystallogr., Sect. F: Struct. Biol. Cryst. Commun.*, 2013, **69**, 821–826.
13 S. Majeed, G. Ofek, A. Belachew, C. C. Huang, T. Q. Zhou and P. D. Kwong, *Structure*, 2003, **11**, 1061–1070.
14 A. McPherson, C. Nguyen, R. Cudney and S. B. Larson, *Cryst. Growth Des.*, 2011, **11**, 1469–1474.
15 C. E. Kundrot, R. A. Judge, M. L. Pusey and E. H. Snell, *Cryst. Growth Des.*, 2001, **1**, 87–99.
16 H. L. Cao, L. H. Sun, J. Li, L. Tang, H. M. Lu, Y. Z. Guo, J. He, Y. M. Liu, X. Z. Xie, H. F. Shen, C. Y. Zhang, W. H. Guo, L. J. Huang, P. Shang, J. H. He and D. C. Yin, *Acta Crystallogr., Sect. D: Biol. Crystallogr.*, 2013, **69**, 1901–1910.
17 D. C. Yin, *Prog. Cryst. Growth Charact. Mater.*, 2015, **61**, 1–26.
18 H. Koizumi, S. Uda, K. Fujiwara and J. Nozawa, *Langmuir*, 2011, **27**, 8333–8338.
19 M. Yaoi, H. Aadachi, K. Takano, H. Matsumura, T. Inoue, Y. Mori and T. Sasaki, *Jpn. J. Appl. Phys.*, 2004, **43**, L686.
20 S. Guha, S. L. Perry, A. S. Pawate and P. J. A. Kenis, *Sens. Actuators, B*, 2012, **174**, 1–9.
21 Y. Liu, X. F. Zhang, C. Y. Zhang, Y. Z. Guo, S. X. Xie, R. B. Zhou, Q. D. Cheng, E. K. Yan, Y. L. Liu, X. L. Lu, Q. Q. Lu, H. M. Lu, Y. J. Ye and D. C. Yin, *CrystEngComm*, 2015, **17**, 5488–5495.
22 E. Saridakis and N. E. Chayen, *Trends Biotechnol.*, 2009, **27**, 99–106.
23 A. Mcpherson and P. Shlichta, *Science*, 1988, **239**, 385–387.
24 S. V. Akella, *Citeseer*, 2014.
25 P. G. Vekilov, *Cryst. Growth Des.*, 2010, **10**, 5007–5019.
26 A. M. Kierzek and P. Zielenkiewicz, *Biophys. Chem.*, 2001, **91**, 1–20.
27 D. Erdemir, A. Y. Lee and A. S. Myerson, *Acc. Chem. Res.*, 2009, **42**, 621–629.
28 M. A. Vorontsova, D. Maes and P. G. Vekilov, *Faraday Discuss.*, 2015, **179**, 27–40.
29 K. G. Soga, J. R. Melrose and R. C. Ball, *J. Chem. Phys.*, 1999, **110**, 2280–2288.
30 V. Talanquer and D. W. Oxtoby, *J. Chem. Phys.*, 1998, **109**, 223–227.
31 P. R. ten Wolde and D. Frenkel, *Science*, 1997, **277**, 1975–1978.
32 D. Vivares, E. W. Kaler and A. M. Lenhoff, *Acta Crystallogr., Sect. D: Biol. Crystallogr.*, 2005, **61**, 819–825.
33 O. Galkin, K. Chen, R. L. Nagel, R. E. Hirsch and P. G. Vekilov, *Proc. Natl. Acad. Sci. U. S. A.*, 2002, **99**, 8479–8483.
34 D. N. Petsev, X. Wu, O. Galkin and P. G. Vekilov, *J. Phys. Chem. B*, 2003, **107**, 3921–3926.
35 M. Muschol and F. Rosenberger, *J. Chem. Phys.*, 1997, **107**, 1953–1962.
36 Y. Li, V. Lubchenko, M. A. Vorontsova, L. Filobelo and P. G. Vekilov, *J. Phys. Chem. B*, 2012, **116**, 10657–10664.
37 Y. Li, V. Lubchenko and P. G. Vekilov, *Rev. Sci. Instrum.*, 2011, **82**, 053106.
38 M. Sleutel and A. E. Van Driessche, *Proc. Natl. Acad. Sci. U. S. A.*, 2014, **111**, E546–E553.
39 W. Pan, O. Galkin, L. Filobelo, R. L. Nagel and P. G. Vekilov, *Biophys. J.*, 2007, **92**, 267–277.
40 V. Uzunova, W. Pan, V. Lubchenko and P. G. Vekilov, *Faraday Discuss.*, 2012, **159**, 87–104.
41 W. Pan, A. B. Kolomeisky and P. G. Vekilov, *J. Chem. Phys.*, 2005, **122**, 174905.
42 J. Savage and A. Dinsmore, *Phys. Rev. Lett.*, 2009, **102**, 198302.
43 N. E. Chayen, E. Saridakis and R. P. Sear, *Proc. Natl. Acad. Sci. U. S. A.*, 2006, **103**, 597–601.
44 T. Kovacs and H. K. Christenson, *Faraday Discuss.*, 2012, **159**, 123–138.
45 D. Gebauer, M. Kellermeier, J. D. Gale, L. Bergström and H. Cölfen, *Chem. Soc. Rev.*, 2014, **43**, 2348–2371.
46 D. Gebauer and H. Cölfen, *Nano Today*, 2011, **6**, 564–584.
47 S. Fermani, C. Vettraino, I. Bonacini, M. Marcaccio, G. Falini, J. A. Gavira and J. M. G. Ruiz, *Cryst. Growth Des.*, 2013, **13**, 3110–3115.
48 J. M. Garcıa-Ruiz, *J. Struct. Biol.*, 2003, **142**, 22–31.
49 E. M. Pouget, P. H. H. Bomans, J. A. C. M. Goos, P. M. Frederik, G. de With and N. A. J. M. Sommerdijk, *Science*, 2009, **323**, 1455–1458.
50 G. Tosi, S. Fermani, G. Falini, J. A. Gavira and J. M. G. Ruiz, *Cryst. Growth Des.*, 2011, **11**, 1542–1548.
51 T. E. Paxton, A. Sambanis and R. W. Rousseau, *J. Cryst. Growth*, 1999, **198**, 656–660.
52 C. N. Nanev, *Cryst. Growth Des.*, 2007, **7**, 1533–1540.
53 C. N. Nanev, *Cryst. Res. Technol.*, 2007, **42**, 4–12.
54 S. Khurshid, E. Saridakis, L. Govada and N. E. Chayen, *Nat. Protoc.*, 2014, **9**, 1621–1633.
55 E. Pechkova, F. Vasile, R. Spera, S. Fiordoro and C. Nicolini, *J. Synchrotron Radiat.*, 2005, **12**, 772–778.
56 E. Saridakis and N. E. Chayen, *Trends Biotechnol.*, 2013, **31**, 515–520.
57 Y.-X. Liu, X.-J. Wang, J. Lu and C.-B. Ching, *J. Phys. Chem. B*, 2007, **111**, 13971–13978.
58 P. D. S. Stewart, S. A. Kolek, R. A. Briggs, N. E. Chayen and P. F. M. Baldock, *Cryst. Growth Des.*, 2011, **11**, 3432–3441.
59 C. Oswald, S. H. J. Smits, E. Bremer and L. Schmitt, *Int. J. Mol. Sci.*, 2008, **9**, 1131–1141.
60 A. D'Arcy, A. Mac Sweeney and A. Haber, *Acta Crystallogr., Sect. D: Biol. Crystallogr.*, 2003, **59**, 1343–1346.
61 T. Bergfors, *J. Struct. Biol.*, 2003, **142**, 66–76.
62 S. Khurshid, L. F. Haire and N. E. Chayen, *J. Appl. Crystallogr.*, 2010, **43**, 752–756.
63 A. D'Arcy, V. A. Frederic and M. Marsh, *Acta Crystallogr., Sect. D: Biol. Crystallogr.*, 2007, **63**, 550–554.
64 E. A. Stura and I. A. Wilson, *J. Cryst. Growth*, 1991, **110**, 270–282.
65 M. Till, A. Robson, M. J. Byrne, A. V. Nair, S. A. Kolek, P. D. S. Stewart and P. R. Race, *J. Visualized Exp.*, 2013, e50548.
66 J. A. Gavira, M. Hernandez-Hernandez, L. A. Gonzalez-Ramirez, R. A. Briggs, S. A. Kolek and P. D. Shaw Stewart, *Cryst. Growth Des.*, 2011, **11**, 2122–2126.
67 S. A. Kolek, B. Braeuning and P. Shaw Stewart, *Acta Crystallogr., Sect. F: Struct. Biol. Commun.*, 2016, **72**, 307–312.

Published on 25 January 2017. Downloaded on 9/24/2024 11:26:54 PM.

68 T. S. Walter, E. J. Mancini, J. Kadlec, S. C. Graham, R. Assenberg, J. Ren, S. Sainsbury, R. J. Owens, D. I. Stuart and J. M. Grimes, *Acta Crystallogr., Sect. F: Struct. Biol. Cryst. Commun.*, 2008, **64**, 14–18.
69 C. Oswald, S. H. Smits, E. Bremer and L. Schmitt, *Int. J. Mol. Sci.*, 2008, **9**, 1131–1141.
70 G. Obmolova, T. J. Malia, A. Teplyakov, R. W. Sweet and G. L. Gilliland, *Acta Crystallogr., Sect. F: Struct. Biol. Commun.*, 2014, **70**, 1107–1115.
71 P. D. Shaw Stewart, S. A. Kolek, R. A. Briggs, N. E. Chayen and P. F. Baldock, *Cryst. Growth Des.*, 2011, **11**, 3432–3441.
72 A. S. Thakur, G. Robin, G. Guncar, N. F. W. Saunders, J. Newman, J. L. Martin and B. Kobe, *PLoS One*, 2007, **2**(10), e1091.
73 D. G. Georgieva, M. E. Kuil, T. H. Oosterkamp, H. W. Zandbergen and J. P. Abrahams, *Acta Crystallogr., Sect. D: Biol. Crystallogr.*, 2007, **63**, 564–570.
74 G. Tosi, S. Fermani, G. Falini, J. A. G. Gallardo and J. M. G. Ruiz, *Acta Crystallogr., Sect. D: Biol. Crystallogr.*, 2008, **64**, 1054–1061.
75 R. P. Sear, *J. Phys.: Condens. Matter*, 2007, **19**(3), 033101.
76 K. Ino, I. Udagawa, K. Iwabata, Y. Takakusagi, M. Kubota, K. Kurosaka, K. Arai, Y. Seki, M. Nogawa, T. Tsunoda, F. Mizukami, H. Taguchi and K. Sakaguchi, *PLoS One*, 2011, **6**(7), e22582.
77 L. Rong, H. Komatsu and S. Yoda, *J. Cryst. Growth*, 2002, **235**, 489–493.
78 C. Y. Zhang, H. F. Shen, Q. J. Wang, Y. Z. Guo, J. He, H. L. Cao, Y. M. Liu, P. Shang and D. C. Yin, *Int. J. Mol. Sci.*, 2013, **14**, 12329–12345.
79 S. Fermani, G. Falini, M. Minnucci and A. Ripamonti, *J. Cryst. Growth*, 2001, **224**, 327–334.
80 N. E. Chayen, E. Saridakis, R. El-Bahar and Y. Nemirovsky, *J. Mol. Biol.*, 2001, **312**, 591–595.
81 P. Asanithi, E. Saridakis, L. Govada, I. Jurewicz, E. W. Brunner, R. Ponnusamy, J. A. S. Cleaver, A. B. Dalton, N. E. Chayen and R. P. Sear, *ACS Appl. Mater. Interfaces*, 2009, **1**, 1203–1210.
82 U. V. Shah, D. R. Williams and J. Y. Y. Heng, *Cryst. Growth Des.*, 2012, **12**, 1362–1369.
83 F. Kertis, S. Khurshid, O. Okman, J. W. Kysar, L. Govada, N. Chayen and J. Erlebacher, *J. Mater. Chem.*, 2012, **22**, 21928–21934.
84 Y. Z. Guo, L. H. Sun, D. Oberthuer, C. Y. Zhang, J. Y. Shi, J. L. Di, B. L. Zhang, H. L. Cao, Y. M. Liu, J. Li, Q. Wang, H. H. Huang, J. Liu, J. M. Schulz, Q. Y. Zhang, J. L. Zhao, C. Betzel, J. H. He and D. C. Yin, *Sci. Rep.*, 2014, DOI: 10.1038/srep07308.
85 U. V. Shah, J. V. Parambil, D. R. Williams, S. J. Hinder and J. Y. Y. Heng, *Powder Technol.*, 2015, **282**, 10–18.
86 A. J. Page and R. P. Sear, *Phys. Rev. Lett.*, 2006, **97**(6), 065701.
87 J. A. van Meel, R. P. Sear and D. Frenkel, *Phys. Rev. Lett.*, 2010, **105**(20), 205501.
88 A. M. Streets and S. R. Quake, *Phys. Rev. Lett.*, 2010, **104**(17), 178102.
89 D. N. Lu, Z. Liu and J. Z. Wu, *Biophys. J.*, 2006, **90**, 3224–3238.
90 E. Pechkova and C. Nicolini, *J. Cryst. Growth*, 2001, **231**, 599–602.
91 E. Pechkova, N. Bragazzi, M. Bozdaganyan, L. Belmonte and C. Nicolini, *Crit. Rev. Eukaryotic Gene Expression*, 2014, **24**, 325–339.
92 E. Pechkova, S. Fiordoro, F. Barbieri and C. Nicolini, *J. Nanomed. Nanotechnol.*, 2014, **5**, 2.
93 E. Pechkova and C. Nicolini, *Nanotechnology*, 2002, **13**, 460–464.
94 E. Pechkova, G. Zanotti and C. Nicolini, *Acta Crystallogr., Sect. D: Biol. Crystallogr.*, 2003, **59**, 2133–2139.
95 E. Pechkova and C. Nicolini, *Anticancer Res.*, 2014, **34**, 6107–6107.
96 E. Pechkova, N. L. Bragazzi and C. Nicolini, *Adv. Protein Chem. Struct. Biol.*, 2014, **95**, 163–191.
97 E. Pechkova, G. Tropiano, C. Riekel and C. Nicolini, *Spectrochim. Acta, Part B*, 2004, **59**, 1687–1693.
98 E. Pechkova and C. Nicolini, *Trends Biotechnol.*, 2004, **22**, 117–122.
99 E. Pechkova, M. Sartore, L. Giacomelli and C. Nicolini, *Rev. Sci. Instrum.*, 2007, **78**(9), 093704.
100 C. Nicolini, L. Belmonte, G. Maksimov, N. Brazhe and E. Pechkova, *J. Microb. Biochem. Technol.*, 2013, **6**, 009–016.
101 C. Nicolini, N. L. Bragazzi, E. Pechkova and R. Lazzari, *J. Proteomics Bioinf.*, 2014, **7**(02), 064–070.
102 M. Bozdaganyan, N. L. Bragazzi, E. Pechkova, K. V. Shaitan and C. Nicolini, *Crit. Rev. Eukaryotic Gene Expression*, 2014, **24**, 311–324.
103 L. Belmonte, E. Pechkova, S. Tripathi, D. Scudieri and C. Nicolini, *Crit. Rev. Eukaryotic Gene Expression*, 2012, **22**, 219–232.
104 E. Pechkova, S. Fiordoro, D. Fontani and C. Nicolini, *Acta Crystallogr., Sect. D: Biol. Crystallogr.*, 2005, **61**, 809–812.
105 C. Nicolini, *Trends Biotechnol.*, 1997, **15**, 395–401.
106 V. I. Troitsky, T. S. Berzina, L. Pastorino, E. Bernasconi and C. Nicolini, *Nanotechnology*, 2003, **14**, 597–602.
107 T. C. Zhou, K. Zhang, T. Kamra, L. Bulow and L. Ye, *J. Mater. Chem. B*, 2015, **3**, 1254–1260.
108 G. Vasapollo, R. D. Sole, L. Mergola, M. R. Lazzoi, A. Scardino, S. Scorrano and G. Mele, *Int. J. Mol. Sci.*, 2011, **12**, 5908–5945.
109 O. Ramstrom and K. Mosbach, *Curr. Opin. Chem. Biol.*, 1999, **3**, 759–764.
110 D. R. Kryscio and N. A. Peppas, *Acta Biomater.*, 2012, **8**, 461–473.
111 C. Alexander, H. S. Andersson, L. I. Andersson, R. J. Ansell, N. Kirsch, I. A. Nicholls, J. O'Mahony and M. J. Whitcombe, *J. Mol. Recognit.*, 2006, **19**, 106–180.
112 D. E. Hansen, *Biomaterials*, 2007, **28**, 4178–4191.
113 A. Bossi, F. Bonini, A. P. F. Turner and S. A. Piletsky, *Biosens. Bioelectron.*, 2007, **22**, 1131–1137.
114 S. Yang, X. Zhang, W. T. Zhao, L. Q. Sun and A. Q. Luo, *J. Mater. Sci.*, 2016, **51**, 937–949.

 This journal is © The Royal Society of Chemistry 2017

115 Q. L. Deng, J. X. Liu, K. G. Yang, Z. Liang, L. H. Zhang and Y. K. Zhang, *Ifpt'6: Progress on Post-Genome Technologies, Proceedings*, 2009, p. 377.
116 S. M. Reddy, Q. T. Phan, H. El-Sharif, L. Govada, D. Stevenson and N. E. Chayen, *Biomacromolecules*, 2012, **13**, 3959–3965.
117 F. Mirata and M. Resmini, *Adv. Biochem. Eng./Biotechnol.*, 2015, **150**, 107–129.
118 P. Lulinski, *Acta Pol. Pharm.*, 2013, **70**, 601–609.
119 I. Chianella, A. Guerreiro, E. Moczko, J. S. Caygill, E. V. Piletska, I. M. P. D. Sansalvador, M. J. Whitcombe and S. A. Piletsky, *Anal. Chem.*, 2013, **85**, 8462–8468.
120 E. Saridakis, S. Khurshid, L. Govada, Q. Phan, D. Hawkins, G. V. Crichlow, E. Lolis, S. M. Reddy and N. E. Chayen, *Proc. Natl. Acad. Sci. U. S. A.*, 2011, **108**, 11081–11086.
121 M. J. Whitcombe, *Nat. Chem.*, 2011, **3**, 657–658.
122 S. Khurshid, L. Govada, H. F. El-Sharif, S. M. Reddy and N. E. Chayen, *Acta Crystallogr., Sect. D: Biol. Crystallogr.*, 2015, **71**, 534–540.
123 Y. F. Hu, Z. H. Chen, Y. J. Fu, Q. Z. He, L. Jiang, J. G. Zheng, Y. N. Gao, P. C. Mei, Z. Z. Chen and X. Q. Ren, *Nat. Commun.*, 2015, **6**, DOI: 10.1038/ncomms7634.
124 Y. Xing, Y. F. Hu, L. Jiang, Z. D. Gao, Z. H. Chen, Z. Z. Chen and X. Q. Ren, *Cryst. Growth Des.*, 2015, **15**, 4932–4937.
125 J.-L. Liao, Y. Wang and S. Hjertén, *Chromatographia*, 1996, **42**, 259–262.
126 H. F. El-Sharif, Q. T. Phan and S. M. Reddy, *Anal. Chim. Acta*, 2014, **809**, 155–161.
127 H. F. EL-Sharif, D. M. Hawkins, D. Stevenson and S. M. Reddy, *Phys. Chem. Chem. Phys.*, 2014, **16**, 15483–15489.
128 K. El Kirat, M. Bartkowski and K. Haupt, *Biosens. Bioelectron.*, 2009, **24**, 2618–2624.

Published on 25 January 2017. Downloaded on 9/24/2024 11:26:54 PM.